Supporting Information

Multiplexed Detection of Attomoles of Nucleic Acids Using 2 Fluorescent Nanoparticle Counting Platform

Xiaojing Pei,[†] Haoyan Yin,[§] Tiancheng Lai,[†] Junlong Zhang,[§] Feng Liu,[†] and Xiao Xu[*,‡], Na Li[*,†]

[†]Beijing National Laboratory for Molecular Sciences (BNLMS), Key Laboratory of Bioorganic Chemistry and Molecular Engineering of Ministry of Education, Institute of Analytical Chemistry, College of Chemistry and Molecular Engineering, Peking University, Beijing, 100871, P. R. China

[§]Beijing National Laboratory for Molecular Sciences, State Key Laboratory of Rare Earth Materials Chemistry and Applications, College of Chemistry and Molecular Engineering, Peking University, Beijing 100871, P. R. China

[‡]Division of Nano Metrology and Materials Measurement, National Institute of Metrology, Beijing, 100029, P. R. China

Corresponding author:

*lina@pku.edu.cn

*xuxiao@pku.edu.cn

Table of contents

1 Experimental Section

1.1 Apparatus

Fluorescence spectra were recorded with a Hitachi F-4500 spectrofluorometer (Hitachi, Japan). The fluorescence images were captured using an Olympus IX73 inverted fluorescence microscope with an Olympus DP80 true colour CCD and Olympus cellSense software (Olympus, Japan). The qRT-PCR was carried out with the ABI 7500 real time PCR System (Applied Biosystems, USA).

1.2 Conjugation of amino-DNA on FNPs

The preparation of the capture DNA conjugated fluorescent nanoparticle (DNA-FNP) was carried out by 1-ethyl-3-(3-(dimethylamino)propyl) carbodiimide hydrochloride (EDC) coupling chemistry. Specifically, 10 μL of 10 mg/mL FNP suspension was washed three times with 100 μL of 50 mM MES buffer (pH 5.0). Then, 10 μL of 50 mg/mL freshly prepared EDC solution was added and mixed, an aliquot (5 μL) of 100 μM amino-DNA was added and mixed by vortexing. The solution with total volume of 100 μL was incubated for 30 min at room temperature with slow agitation, and 10 μL of 50 mg/mL freshly prepared EDC in ice-cold MES buffer was added and mixed well by vortexing. The mixture was stirred overnight and followed centrifugation. Afterward, FNPs were washed three times with 100 μL of 10 mM PBS to remove excess amino-DNA, re-suspended in 1 mL of PBS, and stored at 4 °C for further use.

1.3 Quantification of immobilized DNA on FNPs

Cy3-labeled DNA (5'-NH_2 A_{20}GCAACTAAATTC-Cy3) with sequence the same as that for the immobilization was used in the DNA immobilization step for quantification of the amount of DNA immobilized on FNPs. The procedure for preparing Cy3-DNA-modified FNPs was identical to that described above. Five repetitive centrifugation-washing cycles were carried out after the immobilization to remove excess oligonucleotides. Fluorescence of the solution was measured with the excitation and emission at 540 nm and 562 nm, respectively, and concentration was found from the calibration curve (Figure S3C). The number of oligonucleotides per particle was calculated by dividing the concentration of fluorescent oligonucleotides with the concentration of nanoparticles. All experiments were repeated three times using freshly prepared samples.

1.4 Modification of MBs with biotinylated DNA

The capture DNA functionalized magnetic beads (DNA-MBs) were prepared via streptavidin-biotin conjugation. Specifically, 200 μL of Dynabeads^{TM} magnetic beads were transferred to1 mL of PBS and washed three times with PBS buffer. Then, 25 μL of 100 μM biotinylated DNA (biotin-DNA) was added at room temperature by gentle rotation. After 15 min, the resulting DNA-MBs were washed five times with PBS containing 0.1% Triton X100 to remove the excess biotin-DNA, and re-suspended in 1 mL PBS containing 0.1% Triton X100 and stored at 4 °C for further use.

1.5 Detection of 40-nt TB DNA in the presence of non-target DNA

The detection in the presence of non-target DNAs, including calf thymus DNA (ctDNA) and a 40-nt random sequence (GAGACCATCAATGAGGAAGCTGCA), respectively. The mass ratios of target DNA/ctDNA were varied from 1:0 to 1:10^5. The random sequence was 10 nM. The detection procedure was identical to that described above.

1.6 The selectivity of miR-141 from miR-200 family

The selectivity of miR-141 from members of miR-200 family including miR-200a, miR-200b, miR-200c, miR-429, and miR-141 was carried out in the phosphate buffer saline medium and in 5% HeLa lysate (about 10^6 cells/mL), respectively. Quantification was carried out by following the same procedure as described above with all the miRNAs at the same concentration in a test. And 5 nM, 1 nM as well as 200 pM concentrations were studied in each medium.

1.7 Comparison of miRNA quantification with qRT-PCR

The amount of miR-141 in total RNA extracted from four different cell lines was quantified using a standard miRNA specific quantitative reverse transcript polymerase chain reaction (qRT-PCR) and our proposed method in parallel. The four different cell lines including cervical cancer cell lines (HeLa), hepatocellular carcinoma cell lines (HepG2), breast cancer cell lines (MDA-MB-231), and human breast adenocarcinoma cell line (MCF-7) were incubated by following the same procedures as described above. Total RNA in each kind of cells (approximately 10^6 cells) was extracted using the miRNA isolation kit from Tiangen Biotech (Cat.No. DP501) according to the manufacturer's instruction. The purified RNA extracted from each cells was eluted with RNase-free water and the final volume was 15 μL.

The stem-loop method was applied for reverse transcription methodologies to generate cDNA for miR-141. The reverse transcription reaction was carried out using M-MLV reverse transcriptase (Cat. No. 28025013) from Takara Biotechnology according to manufacturer instructions. The 15 μL RT reaction mixture was composed of 7 μL of RT master mix, 5 μL of total RNA sample (200 ng) or miR-141, and 3 μL of 5× RT primer solution. Each sample was reverse transcribed in triplicate and the blank reaction (no template control) in duplicate. The temperature program for the RT reaction was: 16 °C for 30 min, 60 °C for 30 min, 72 °C for 5 min.

The cDNA was then amplified in a qPCR reaction. The 20 μL of PCR reaction mixture was made of 1 μL of primer 1 (10 pmol/μL), 1 μL of primer 2 (10 pmol/μL), 2 μL of cDNA (RT reaction mixture), 10 μL of SYBR Mix (Roche, Cat. No. 04913914001), 6 μL of nuclease-free water. qPCR reactions were run with an Applied Biosystems 7500 Real time PCR System using the following temperature program: 94 °C for 10 min followed by 45 cycles of 94 °C for 15 s and 60 °C for 60 s, and finally, 72 °C for 10 min.

The qRT-PCR measurements were carried out on 4 different cell lines (3 replicates) as indicated above; the reverse transcription reaction were carried out for each extracted total RNA (3 replicates) and qPCR reactions were run on each cDNA mixture. Quantification was performed using the standard curve method (standards made of synthetic miR-141, serial dilutions from original concentration 10 μM). Relative expression analysis was performed using 2-DeltaDeltaCt calculation based on U6 as the internal reference.

1.8 Simultaneous detection of DNA and miR-21

The simultaneous detection of DNA and miR-21 was carried out with the same procedure as that for nucleic acid detection. The discrimination factors (DFs) is defined as the ratio of the net counting numbers gain obtained with the perfectly matched target sequence to that obtained with the mismatched sequences under the same conditions.

1. TA GTA AGA ATG TAT AGC CCT CCA ACT ACC ACA

2. ACGCCATCAGCT ACC AGC ATT CTG GAC ATA AG

KAS-6A : ACT TGT GGT AGT TGG AGC TGA TGG CGT

1.9 The sequences used in this study

Table S1 Sequences of oligonucleotides used in DNA assay

Sequences		**Description**
HIV -FNP12	A_{20} CAG AAT GCT GGT	5'-NH_2 C_{12}
HIV -FNP 20	A_{20} CT TAT GTC CAG AAT GCT GGT	5'-NH_2 C_{12}
HIV -FNP 30	A_{20} TTG TCT TAT GTC CAG AAT GCT GGT	5'-NH_2 C_{12}
HIV -MB-12	AGG GCT ATA CAT A_{10}	3'-Biotin-TEG
HIV-MB20	AGG GCT ATA CAT TCT TAC TA A_{10}	3'-Biotin-TEG
HIV-MB30	AGG GCT ATA CAT TCT TAC TAT TTT ATT TAA TCC CAG A_{10}	3'-Biotin-TEG
HIV-24	ATG TAT AGC CCT ACC AGC ATT CTG	
HIV40	TA GTA AGA ATG TAT AGC CCT ACC AGC ATT CTG GAC ATA AG	
HIV60	CTG GGA TTA AAT AAA ATA GTA AGA ATG TAT AGC CCT ACC AGC ATT CTG GAC ATA AGA CAA	
TB-FNP 12	A_{20} CCC TGC CCA GGT	5'-NH_2 C_{12}
TB- FNP 20	A_{20} TA GGC GAA CCC TGC CCA GGT	5'-NH_2 C_{12}
TB-FNP 30	A_{20} CAC GTA GGC GAA CCC TGC CCA GGT	5'-NH_2 C_{12}
TB-MB-12	CGA CAC ATA GGT A_{10}	3'-Biotin-TEG
TB-MB-20	CGA CAC ATA GGT GAG GTC TG A_{10}	3'-Biotin-TEG
MB-TB	CGA CAC ATA GGT GAG GTC TGC TAC CCA CAG CCG GTT A_{10}	3'-Biotin-TEG
TB-24	ACC TAT GTG TCG ACC TGG GCA GGG	
TB-40	CA GAC CTC ACC TAT GTG TCG ACC TGG GCA GGG TTC GCC TA	
TB-60	AAC CGG CTG TGG GTA GCA GAC CTC ACC TAT GTG TCG ACC TGG GCA GGG TTC GCC TAC GTG	
FNP-HBV-20	A_{20} AT CGG TCC TGT TTA ACC TCC	5'-NH_2 C_{12}
FNP -HBV	A_{20} GCG TAT CGG TCC TGT TTA ACC TCC	5'-NH_2 C_{12}
MB-HBV-20	TGT TCT CCA A CC CCG CAG AC A_{10}	3'-Biotin-TEG

MB-HBV	TGT TCT CCA A CC CCG CAG ACA CAT CCA GCG ATA GCC A_{10}	3'-Biotin-TEG
HBV-40	GT CTG CGG GGT TGG AGA ACA GGA GGT TAA ACA GGA CCG AT	
HBV-60	GGC TAT CGC TGG ATG TGT CTG CGG GGT TGG AGA ACA GGA GGT TAA ACA GGA CCG ATA CGC	

Table S2 Sequences of oligonucleotides used in miRNA assay

Oligonucleotides	Sequences
miR-21	Target: UAGCUUAUCAGACUGAUGUUG Capture DNA: ACTGATAAGCTA A_{10} Probe DNA: A_{20} TCAACATCAGT
miR let 7c	Target: UGA GGU AGU AGG UUG UAU GGU U Capture DNA: CT ACT ACC TCA A_{10} Probe DNA: A_{20} ACC ATA CAA C
miR-141	Target: UAACACUGUCUGGUAAAGAUGG Capture DNA: AGACAGTGTT A_{10} Probe DNA: A_{20}CCATCTTTACC
miR-200a	UAA CAC UGU CUG GUA ACG AUG U
miR-200b	UAA UAC UGC CUG GUA AUG AUG A
miR-200c	UAA UAC UGC CGG GUA AUG AUG A
miR-429	UAA UAC UGU CUG GUA AAA CCG U

Table S3 Sequences of oligonucleotides used in DNA and miRNA

Oligonucleotides	Sequences	Description
K-Ras gene	TAG TTG GAG CTG GTG GCG TAG GCA	
FNP- *K-Ras* gene	A_{20}TGC CTA CGC CAC	5'-NH_2 C_{12}
MB- *K-Ras* gene	CAG CTC CAA CTA A_{10}	3'-Biotin-TEG
miR-21	UAGCUUAUCAGACUGAUGUUG	
Capture DNA	ACTGATAAGCTA A_{10}	3'-Biotin-TEG
Probe DNA	A_{20} TCAACATCAGT	5'-NH_2 C_{12}
MT-1	TAG TTG GAG CTG A*TG GCG TAG GCA	
MT-2	TAG TTG GAG CTG ATG ACG TAG GCA	
MT-3	TAG TTG GAA CTG ATG ACG TAG GCA	

* The mutated bases in the *K-Ras* gene.

Table S4 Sequences of oligonucleotides used RT-PCR assay

Oligonucleotides	Sequences
Forward primer for U6	GCTTCGGCAGCACATATACTAAAAT
Reverse primer for U6	CGCTTCACGAATTTGCGTGTCAT
Reverse primer for miR-141	GCAGGGTCCGAGGTATTC
Reverse transcription primer for miR-141	GTCGTATCCAGTGCAGGGTCCGAGGTATTCG CACTGGATACGACCCATCTTT
Forward primer for miR-141	ATGGTTCGTGCGTAACACTGTCTGGTAAA

2 Supplemental results

2.1 Optimization of the DNA density of MBs and FNPs

As shown in Figure S1, 0.8 μM DNA for 200 μL of 2 mg/mL MBs and 0.04 μM for 50 μL 2.9×10^2 fM FNPs were selected for the subsequent study. It was confirmed that there were approximately 2.4×10^3 strands on one 200-nm FNP and about 8.1 $x10^3$ strands on one 1-μm MB.

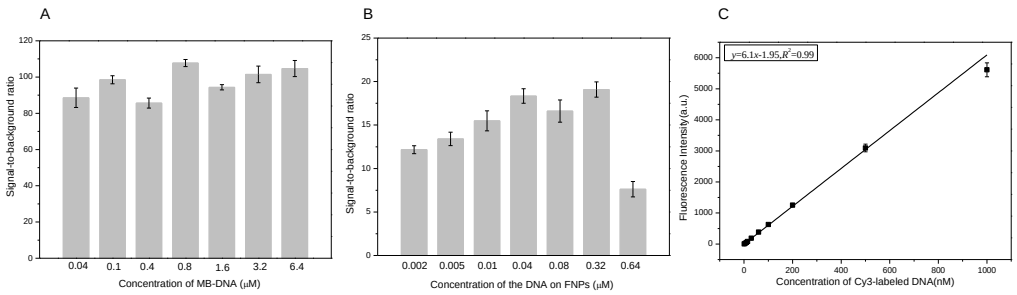

Figure S1 The concentration of biotin-DNA were added for modifying MBs (A); the concentration of amino-DNA were added for conjugating the FNPs (B); the 40 μL of 2 mg/mL MBs and 10 μL of 29 fM green FNPs, and 2 nM 40-nt TB DNA were applied, respectively. The calibration curve of Cy3-labeled DNA (C).

2.2 Optimization of the amount of DNA-FNPs and DNA-MBs

To improve the sensitivity of the assay, the volume of DNA-FNPs and DNA-MBs in the test system were optimized using the 500 pM 40-nt TB DNA. As shown in Figure S2, the 40 μL of 2 mg/mL MBs and 10 μL of 2.92 pM green FNPs, 20 μL of 2.92 pM red FNPs and 20 μL of 3.98 pM blue FNPs were determined, respectively, according to the signal-to-background ratio performance.

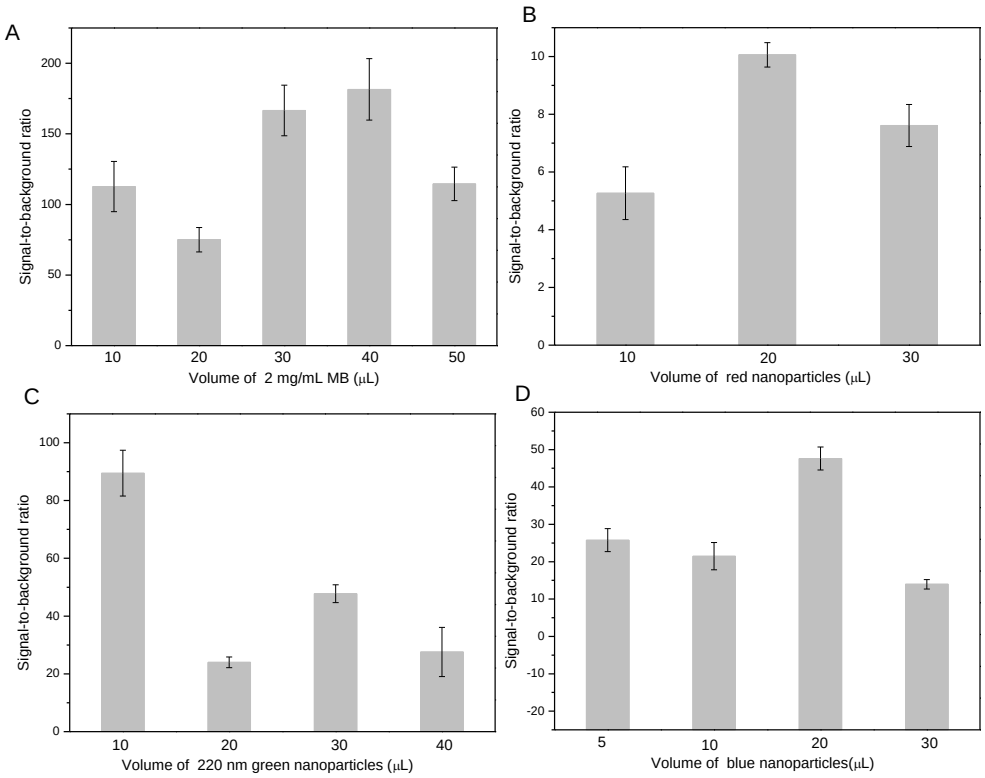

Figure S2 Optimization of experimental conditions: for the volume of DNA-MBs, using green FNPs and 2 nM 40-nt TB DNA (A); for red DNA-FNPs, using 500 pM 40-nt HIV DNA (B); for green DNA-FNPs, using 500 pM 40-nt TB DNA (C); for blue DNA-FNPs, using 500 pM 40-nt HBV DNA in the detection system (D).

2.3 Optimization of surfactants for the assay

A number of surfactants were evaluated to reduce undesired non-specific interactions with MBs. The 0.1% SDS has been reported to inhibit non-specific interactions with proteins and nucleic acids detections, but the signal fluctuation in this experiment jeopardized the assay reproducibility. The signals were highest with 0.1% Triton X-100, the non-ionic surfactant, thus was used throughout the assay (**Figure S3)**.

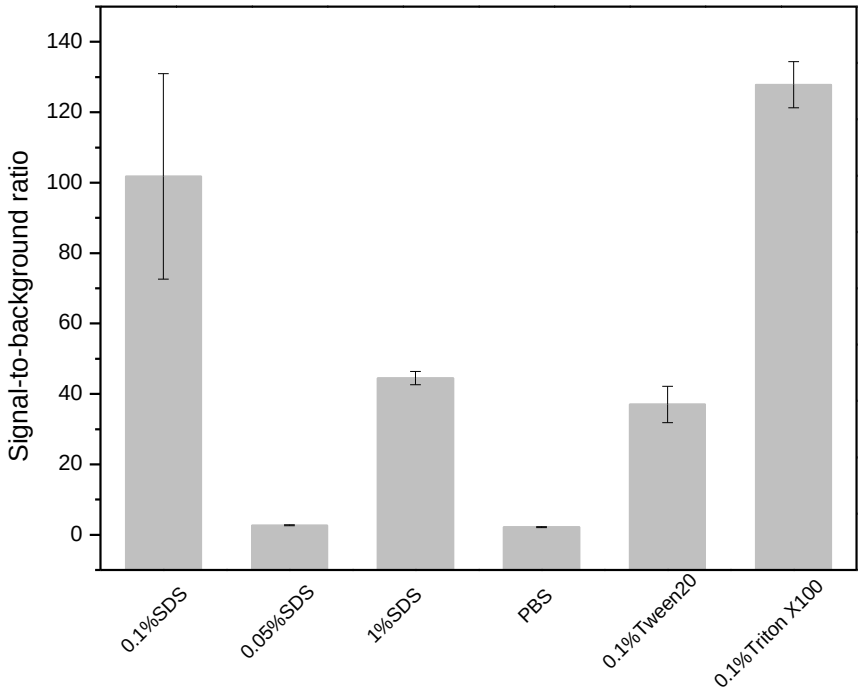

Figure S3 Surfactants tested to reduce non-specific binding for the assay, the 40 μL of 2 mg/mL MBs, 10 μL of 29 fM green FNPs, and 2 nM 40-nt TB DNA were applied, respectively.

2.4 Optimization of the reaction time and the dehybridization time by NaOH

The sandwich structure amongst DNA-MB, target, and DNA-FNP was formed in sequence by first incubating DNA-MB with target, and then with DNA-FNPs. The total incubation time was the sum of the time course associated with each period of incubation, and the following combinations were tested, 0.5 +1 h, 1+1 h, and 1+2 h. As shown in **FigureS4,** the 1+2 pattern was chose for subsequent study. Moreover, the time of NaOH to unwind the sandwich assembly was also optimized. Compared with 10 min thermal dissociation at 75 °C, the NaOH dissociation is more effective; however, the chemical structure of FNPs might change for the long time immersing in the NaOH environment. Therefore, the 15 min NaOH dissociation was adopted.

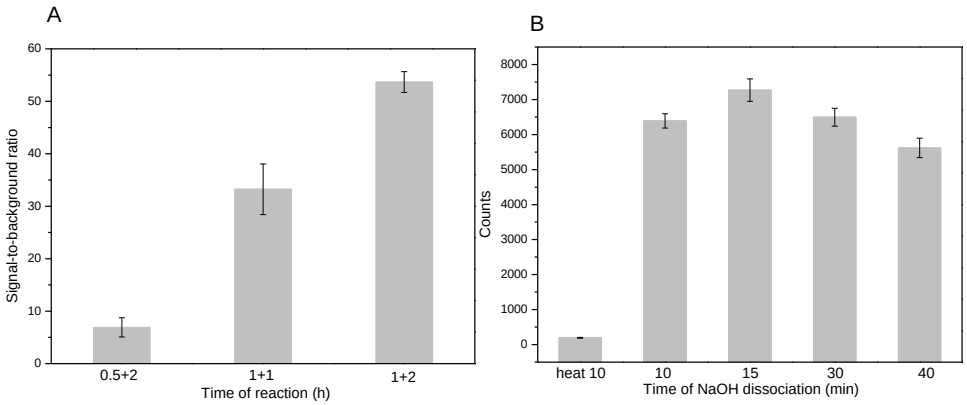

Figure S4 Optimization of the reaction time (A), and the time of NaOH dissociation (B). The 40 μL of 2 mg/mL MBs, 10 μL of 29 fM green FNPs, and 2 nM 40-nt TB DNA were applied, respectively.

2.5 Results on green FNPs by the proposed platform and spectrofluorometry

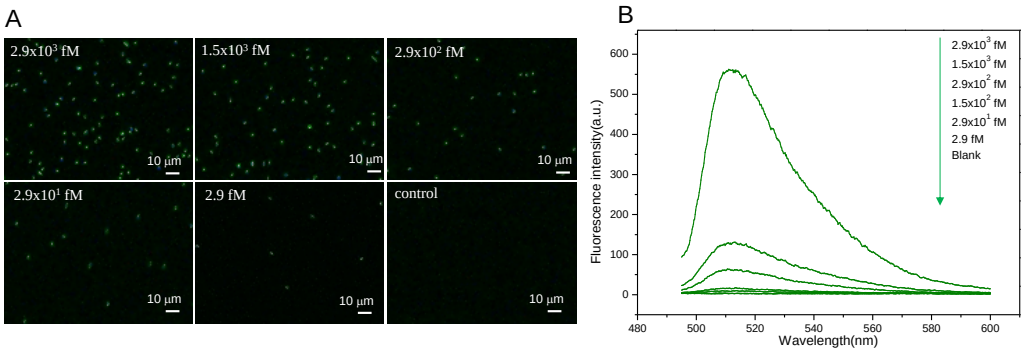

Figure S5 Fluorescence microscopic images of green FNPs at different dilution levels (A); fluorescence spectra of green FNPs at different dilution levels (B).

Table S5 The automatic counting rate compared with manual counting.

Manual	Automatic	Accuracy
2321	2220	96%
347	338	97%
328	316	96%
107	106	99%
116	117	100%
57	57	100%

2.6 Detection of 40-nt TB DNA by the proposed counting platform and flow cytometry

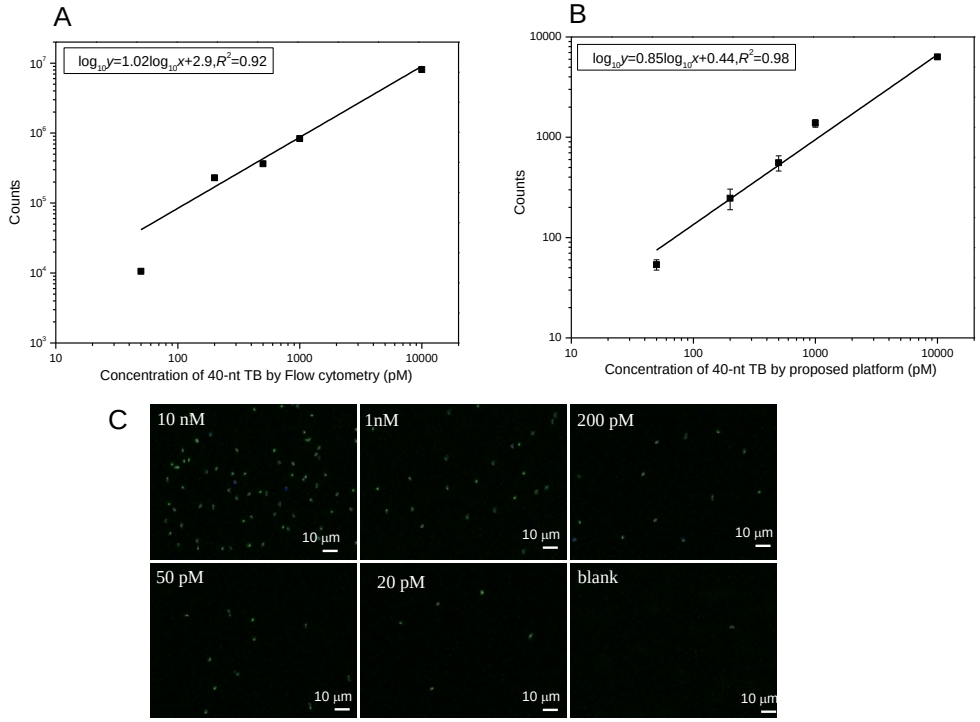

Figure S6 Calibration curves of 40-nt TB DNA by the proposed platform (A) and by flow cytometry (B); fluorescence microscopic images of FNPs associated with the concentration of 40-nt TB DNA (C). The 40 μL of 2 mg/mL MBs and 10 μL of 29 fM green FNPs were applied, respectively.

2.7 Detection of TB DNA of different lengths with 20-nt and 30-nt capture DNA

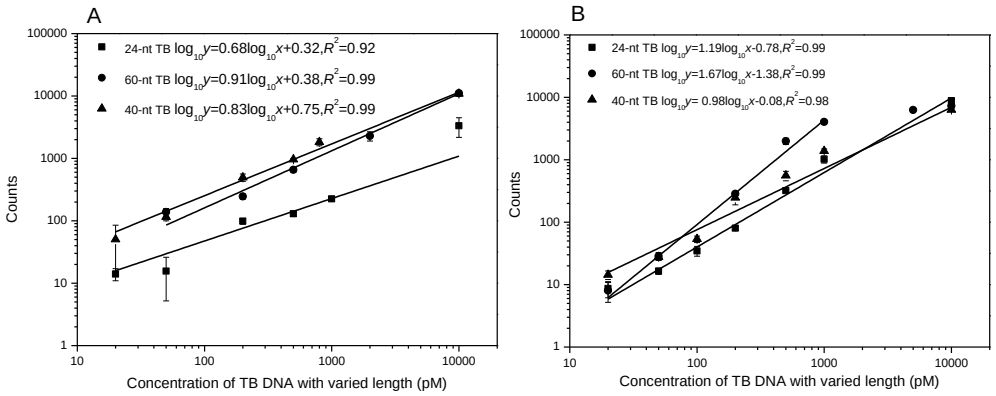

Figure S7 Calibration curves of 24-nt, 40-nt, and 60-nt TB DNA using the 30-nt (A) and 20-nt (B) capture DNA, respectively. The 40 μL of 2 mg/mL MBs and 10 μL of 29 fM green FNPs were applied, respectively.

Table S6 The spike recovery of three 40-nt DNA targets in the cross reactivity study.

500 pM	HBV	TB	HIV
Spike recovery (%)	114.9±8.4	102.6±1.7	101.8±7.5

2.8 Detection of 60-nt DNA targets

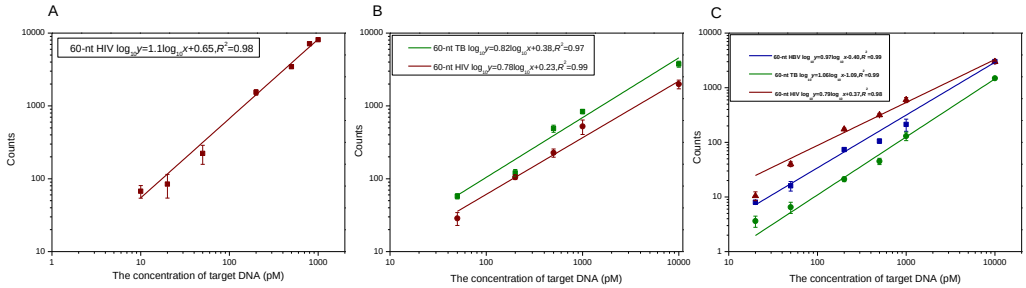

Figure S8 Calibration curves for 60-nt HIV DNA (A), the mixture of 60-nt TB and HIV DNAs (B), as well as the mixture of 60-nt TB, HBV, and HIV DNAs (C) with 30-nt capture DNA. The 40 μL of 2 mg/mL MBs and 10 μL of 2.92 pM green FNPs, 20 μL of 2.92 pM red FNPs and 20 μL of 3.98 pM blue FNPs were applied, respectively.

2.9 Detection of TB DNA in the presence of non-target DNA

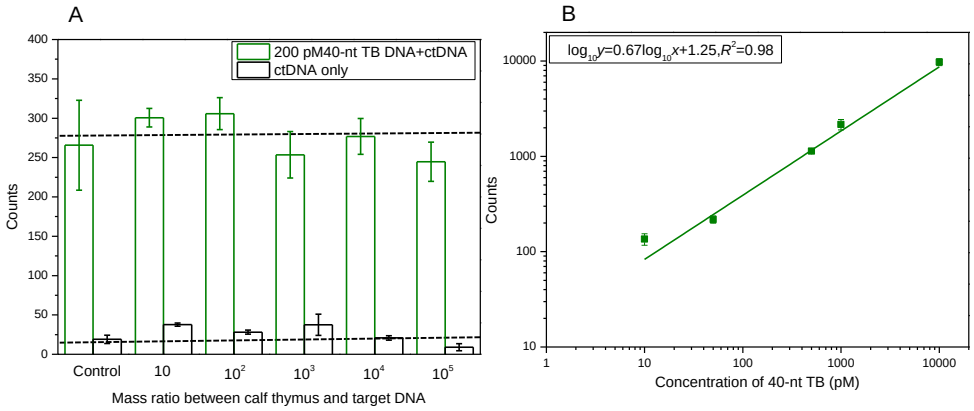

Figure S9 Counting results of 40-nt TB DNA in the presence of increasing amounts of ctDNA (A), the dashed lines denote the average of reagent background and the signal from 200 pM TB DNA, respectively; calibration curve of 40-nt TB DNA in the presence of 10 nM random sequences (B). The 40 μL of 2 mg/mL MBs and 10 μL of 2.92 pM green FNPs were applied, respectively.

2.10 The qRT-PCR quantification results

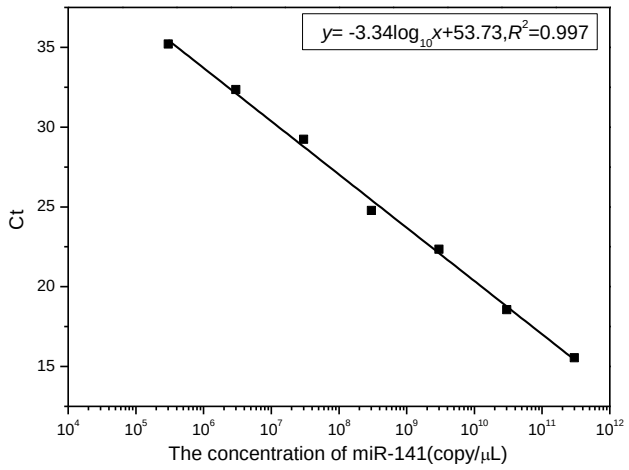

Figure S10 The calibration curve of qRT-PCR quantification for miR-141.

Table S7 The comparation between the miR-141 amount in four cell lines by the proposed countingplatform and qRT-PCR.

miR-141(copies/ng total RNA)	the proposed platform	qRT-PCR
MDA-MB-231	$(2.46\pm0.06)\times10^5$	$(1.94\pm0.93)\times10^5$
HeLa	$(0.87\pm0.23)\times10^5$	$(1.44\pm0.43)\times10^5$
MCF-7	$(1.84\pm0.19)\times10^5$	$(2.08\pm0.44)\times10^5$
HepG2	$(0.74\pm0.12)\times10^5$	$(1.03\pm0.16)\times10^5$

Table S8 The comparation between the miR-141and miR-21 amount in four cell lines by the proposed counting platform.

miR-141(copies/ng total RNA)	miR-141	miR-21
MDA-MB-231	$(4.39\pm2.52)\times10^5$	$(4.57\pm0.33)\times10^5$
HeLa	$(1.98\pm0.12)\times10^5$	$(3.54\pm2.56)\times10^5$
MCF-7	$(3.64\pm1.26)\times10^5$	$(4.26\pm0.75)\times10^5$
HepG2	$(1.27\pm0.41)\times10^5$	$(1.78\pm0.31)\times10^5$

2.11 Fluorescence microscopic images of DNA detection

The images of **Figure S11−S13** are associated with **Figure 2**.

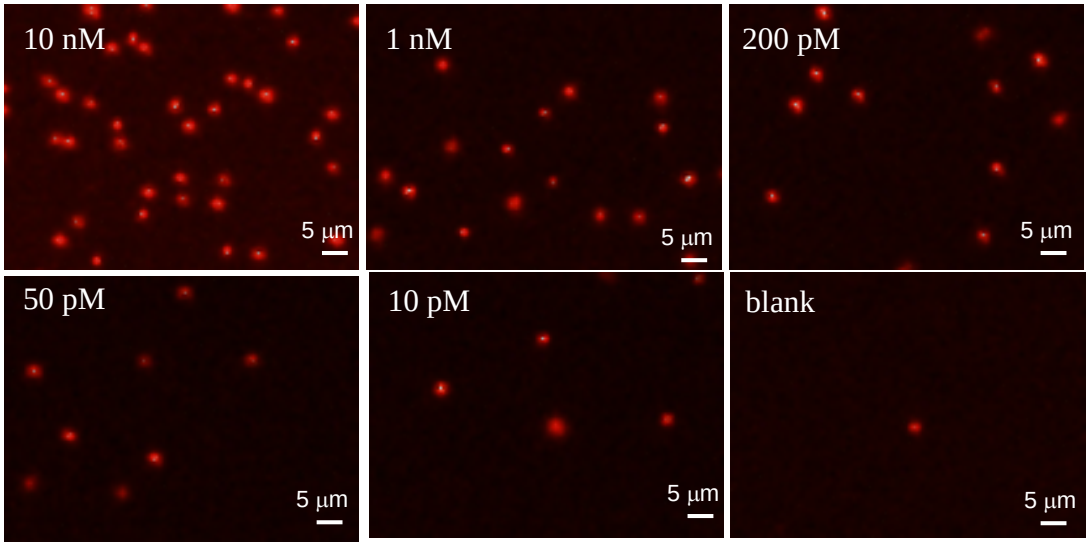

Figure S11 The fluorescence microscopic images of red FNPs with different concentrations of 40-nt HIV DNA in singleplexed detection.

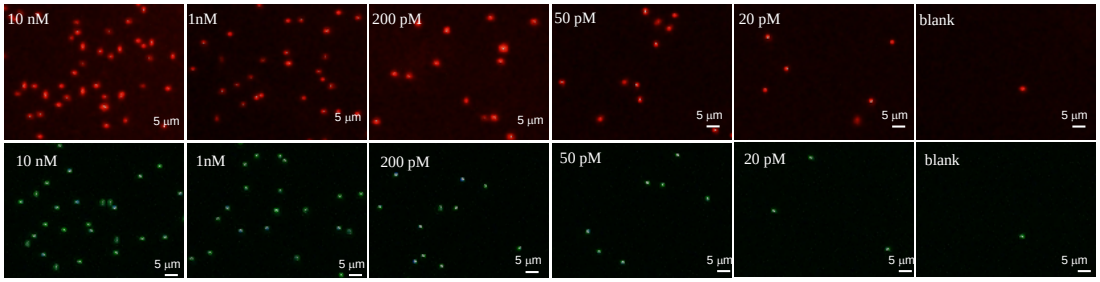

Figure S12 The fluorescence microscopic images of red and green FNPs with different concentrations of 40-nt HIV DNA and TB DNA in duplexed detection.

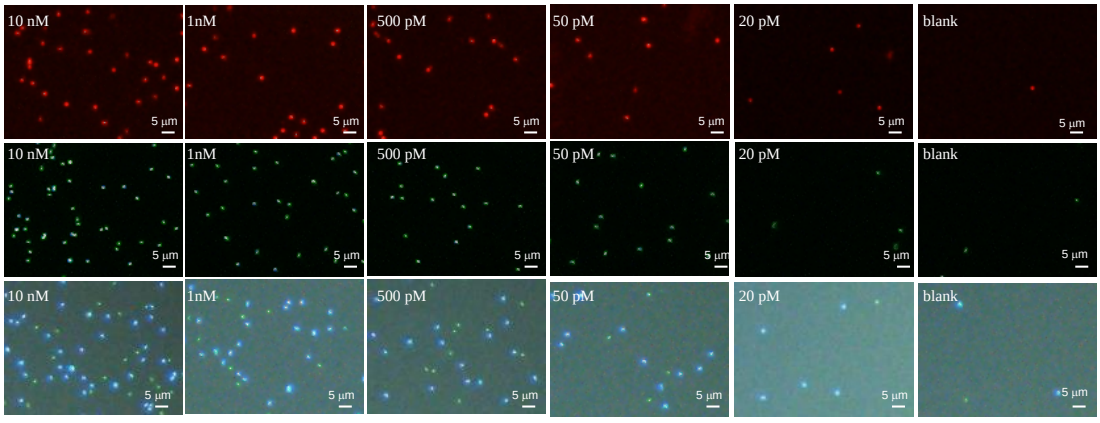

Figure S13 The fluorescence microscopic images of red, green and blue FNPs with different concentrations of 40-nt HIV, TB, and HBV DNA in triplexed detection.

2.12 Fluorescence microscopic images of miRNA detection

The images of **Figure S14−S17** are associated with **Figure 3A−3D**.

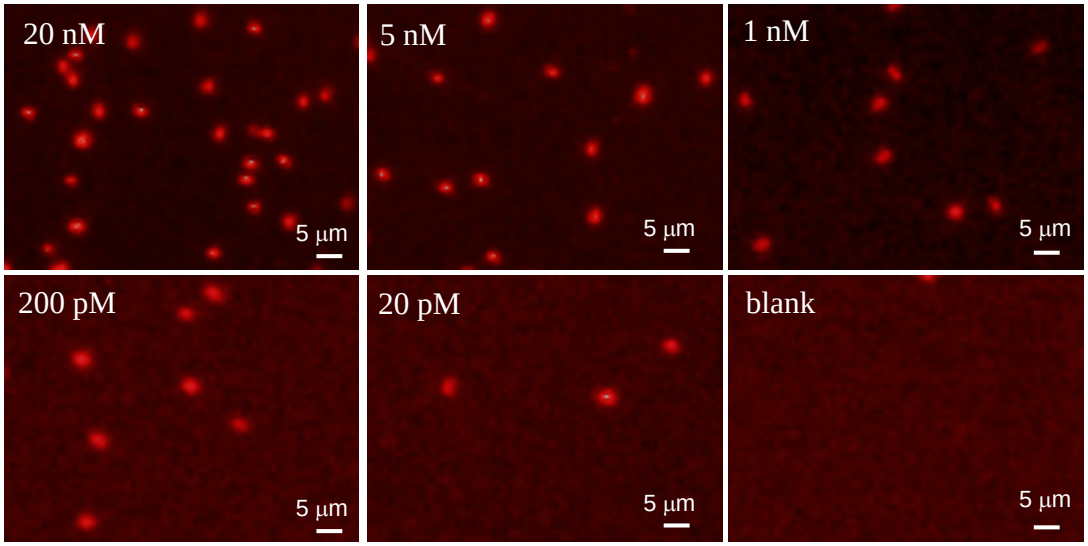

Figure S14 The fluorescence microscopic images of red FNPs with different concentrations of miR-21 in singleplexed detection.

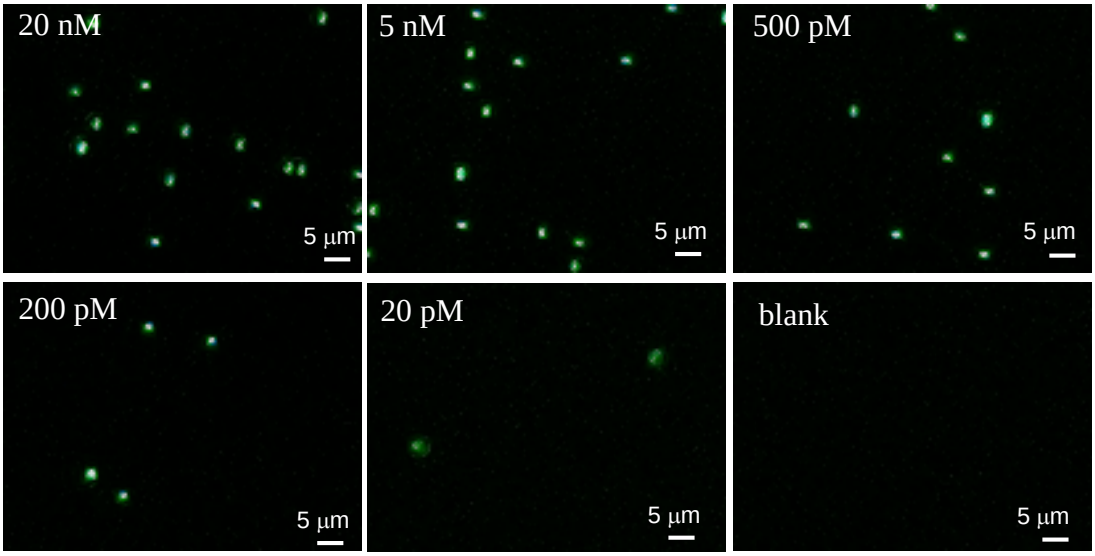

Figure S15 The fluorescence microscopic images of green FNPs with different concentrations of miR-141 in singleplexed detection.

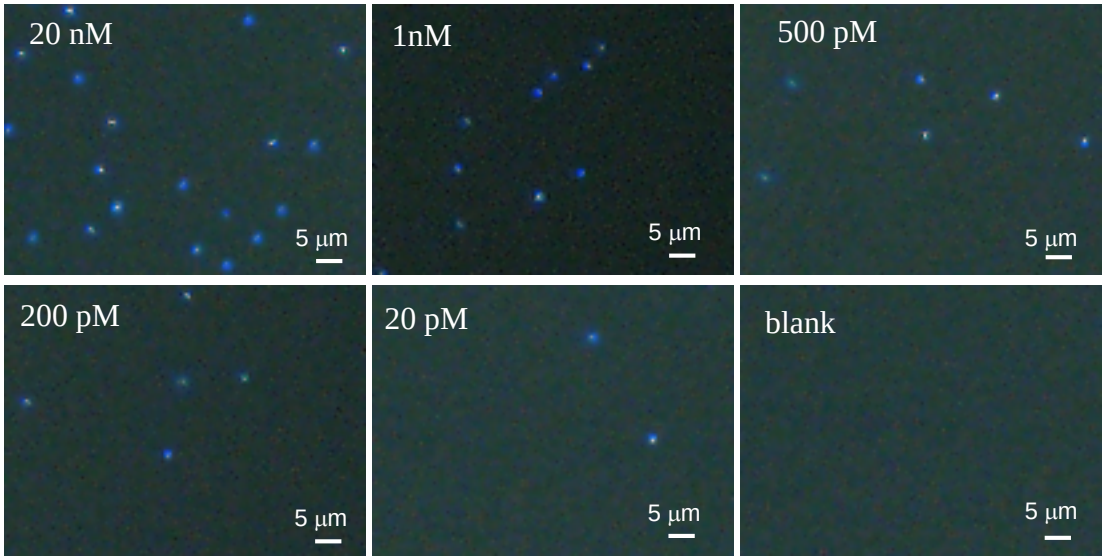

Figure S16 The fluorescence microscopic images of blue FNPs with different concentrations of let-7c in singleplexed detection.

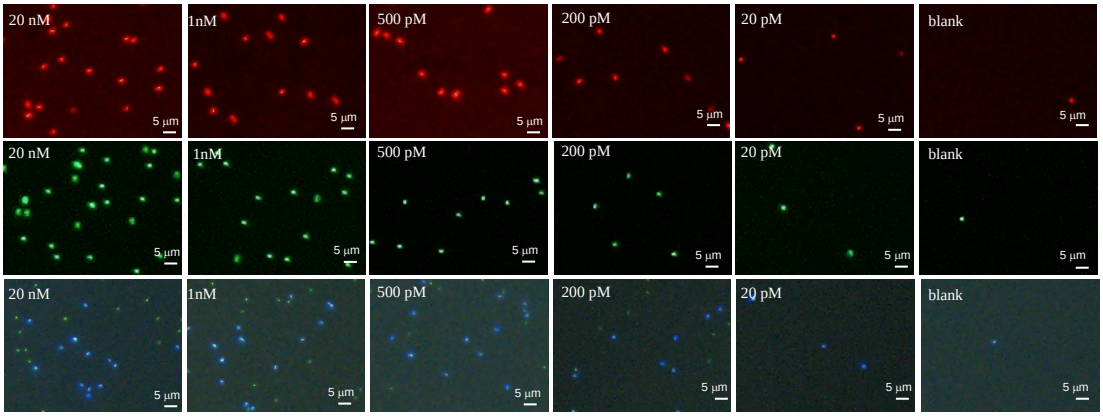

Figure S17 The fluorescence microscopic images of red, green and blue FNPs with different concentrations of miR-21, miR-141, let-7c in triplexed detection.

2.13 Fluorescence microscopic images for duplexed detection of *K-Ras* gene and miR-21

The images of **Figure S18** are associated with **Figure 3E**.

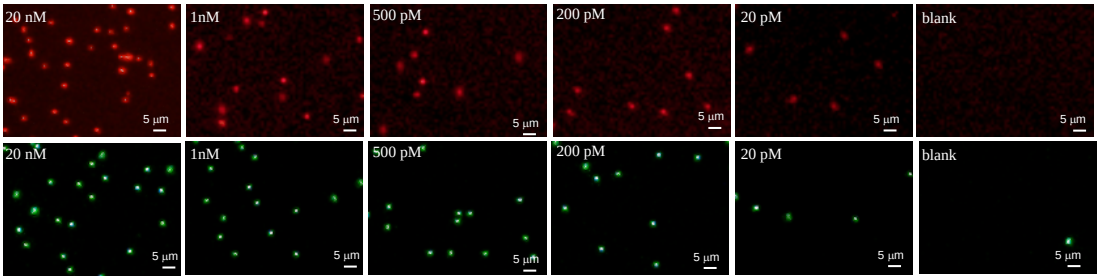

Figure S18 The fluorescence microscopic images of red and green FNPs with different concentrations of *K-Ras* gene and miR-21 detection.

2.14 Comparison with published non-amplification optical methods for multiplexed detection

Table S9 Summary of published non-amplification optical methods for multiplexed detection.

Method	Dynamic range or LOD	Reference
FNP counting	Several pM to a few dozen pM	This work
SERS	Singleplex: miR-21: 50 fM−100 nM miR-122: 10 fM−100 nM miR-223: 50 fM−100 nM Multiplex：miR-21 and miR-223: 10 nM−10 pM, miR-122: 1nM−1 pM	1
SERS and LNA	Singleplex: 100 aM; multiplex:100 pM	2
FRET	Singleplex: 0.02 nM to 10 nM LOD: 18 pM for miR-155,12 pM for miR-182 and 11 pM for miR-197; multiplex potential	3
AuNPs by dark-field microscopy	Multiplex: dynamic range: 3−300 pM LOD: 3 pM−10 pM for 9 miRNA targets	4
Single Molecule Array (Simoa) technique and LNA	Singleplex: miR-16: 0.76 fM; miR-21:1.60 fM; miR-141:0.58 fM; miR-25:27.34 fM; miR-126: 8.94 fM; miR-155:4.37 fM. Multiplex: ~10 fM	5
QDs encoded hydrogel particles	Singleplex: miR-18b: 21.8 amol; miR-342: 8.08 amol; miR-1306: 7.75 amol Multiplex:miR-18b: 25.9 amol; miR-342: 18.6 amol; miR-1306: 10.8 amol	6
Bio-barcode gel assay	Singleplex: aM levels; multiplex:1fM	7
Nano MOFs	Singleplex: 0−1000 nM, LOD:10 pM; multiplex in the cell	8
Nanopore and barcode	Multiplex: 10 pM−200 nM for four miRNAs	9
Silver nanocluster probes	Singleplex: about 1 μM and multiplex potential	10
xMAP Array	Dynamic range: 0.5 pM−2 nM and LOD: 0.5 pM for miRNA21, miRNA222, miRNA20a, and miRNA223;	11
Laser ablation ICP-MS to detect miRNAs on Northern blot membranes	Singleplex: low femtomol range and multiplex potential	12
PNA and Nano Graphene Oxide (PANGO)	Dynamic range: 0−1000 nM; LOD: 1 pM	13
Encoded gel microparticles microfluidic scanner	Multiplex: 1−10000 amol	14
Phage-mediated counting	LOD: multiplex (miR-195 and let-7a)：5 aM	15
Silicon photonic microring resonators	Singleplex: 2 μM−1.95 nM; LOD:~10 nM; multiplex expression levels of four miRNAs in cells	16

3 References

(1) Zhou, W.; Tian, Y.-F.; Yin, B.-C.; Ye, B.-C. *Anal. Chem.* **2017**.

(2) Kang, T.; Kim, H.; Lee, J. M.; Lee, H.; Choi, Y.-S.; Kang, G.; Seo, M.-K.; Chung, B. H.; Jung, Y.; Kim, B. *Small* **2014**, *10*, 4200-4206.

(3) Liu, Y.; Wei, M.; Li, Y.; Liu, A.; Wei, W.; Zhang, Y.; Liu, S. *Anal. Chem.* **2017**, *89*, 3430-3436.

(4) Kim, S.; Park, J.-E.; Hwang, W.; Seo, J.; Lee, Y.-K.; Hwang, J.-H.; Nam, J.-M. *J. Am. Chem. Soc.* **2017**, *139*, 3558-3566.

(5) Cohen, L.; Hartman, M. R.; Amardey-Wellington, A.; Walt, D. R. *Nucleic Acids. Res.* **2017**, e137.

(6) Roh, Y. H.; Sim, S. J.; Cho, I.-J.; Choi, N.; Bong, K. W. *Analyst* **2016**, *141*, 4578-4586.

(7) Lee, H.; Park, J.-E.; Nam, J.-M. *Nat. Commun.* **2014**, *5*, 3367.

(8) Wu, Y.; Han, J.; Xue, P.; Xu, R.; Kang, Y. *Nanoscale* **2015**, *7*, 1753-1759.

(9) Zhang, X.; Wang, Y.; Fricke, B. L.; Gu, L.-Q. *Acs Nano* **2014**, *8*, 3444-3450.

(10) Shah, P.; Thulstrup, P. W.; Cho, S. K.; Bhang, Y.-J.; Ahn, J. C.; Choi, S. W.; Bjerrum, M. J.; Yang, S. W. *Analyst* **2014**, *139*, 2158-2166.

(11) Li, D.; Wang, Y.; Lau, C.; Lu, J. *Anal. Chem.* **2014**, *86*, 10148-10156.

(12) de Bang, T. C.; Shah, P.; Cho, S. K.; Yang, S. W.; Husted, S. *Anal. Chem.* **2014**, *86*, 6823-6826.

(13) Ryoo, S.-R.; Lee, J.; Yeo, J.; Na, H.-K.; Kim, Y.-K.; Jang, H.; Lee, J. H.; Han, S. W.; Lee, Y.; Kim, V. N.; Min, D.-H. *Acs Nano* **2013**, *7*, 5882-5891.

(14) Chapin, S. C.; Appleyard, D. C.; Pregibon, D. C.; Doyle, P. S. *Angew. Chem. Int. Ed.* **2011**, *50*, 2289-2293.

(15) Zhou, X.; Cao, P.; Zhu, Y.; Lu, W.; Gu, N.; Mao, C. *Nature Mater.* **2015**, *14*, 1058-1065.

(16) Qavi, A. J.; Bailey, R. C. *Angew. Chem. Int. Ed.* **2010**, *49*, 4608-4611.